Hydrobiologia
https://doi.org/10.1007/s10750-021-04660-4

PRIMARY RESEARCH PAPER

High-discharge disturbance does not alter the seasonal trajectory of nutrient uptake in a montane stream

Jared A. Balik · Derek C. West · Brad W. Taylor

Received: 10 February 2021 / Revised: 30 June 2021 / Accepted: 4 July 2021
© The Author(s), under exclusive licence to Springer Nature Switzerland AG 2021

Abstract Flood disturbances scour stream benthos and initiate biofilm succession. Nutrient uptake is generally expected to increase over successional time, but succession likely depends on the environmental context and seasonal timing or frequency of flooding. To explore how a midsummer flood alters uptake in streams with predictable snowmelt-driven spring floods followed by typically stable summertime flow, we present two summers of uptake and biofilm trajectories in the East River, a high elevation oligotrophic stream in central Colorado, USA. In 2017, a large rainstorm caused a midsummer flood 3.4 × the previous week's average discharge. Biofilm biomass accrued and areal P uptake increased after the flood. During the same timeframe of 2018 without any midsummer floods, biofilm biomass and P uptake declined. N uptake did not change in either year. The ratio of biofilm chlorophyll-a to ash-free dry mass explained 84% of the variation in N uptake across both years, whereas an additional model term for ambient P explained 96% of the variation in P uptake. Higher proportion of algae was associated with greater uptake of both nutrients, suggesting that algae drive uptake, whereas temperature and light availability did not influence uptake, suggesting that nutrient-limited heterotrophs could also provide important controls.

Keywords Nutrient uptake · Ammonium · Phosphorus · Disturbance · Floods · Biofilm · Algae · Succession · Seasonality

Handling editor: Verónica Ferreira.

Supplementary Information The online version of this article contains supplementary material available (https://doi.org/10.1007/s10750-021-04660-4).

J. A. Balik (✉) · D. C. West · B. W. Taylor
Department of Applied Ecology, North Carolina State University, Raleigh, NC 27695, USA
e-mail: balikj3@gmail.com

J. A. Balik · D. C. West · B. W. Taylor
Rocky Mountain Biological Laboratory, Crested Butte, CO 81224, USA

Introduction

Streams are sensitive to disturbances in their watersheds (Likens et al., 1970). Watershed-scale disturbances often alter stream nutrient regimes, but in some cases nutrient uptake in streams can mediate the effects of disturbance on watershed-scale nutrient transport and processing. For example, although watershed gross nutrient export from Hubbard Brook Forest (NH, USA) increased after an ice storm, net export would have been 55–131% higher if not for simultaneous increases in stream uptake (Bernhardt et al., 2003). Likewise, at Walker Branch (TN, USA), canopy damage alleviated autotroph light limitation and increased uptake (Mulholland et al., 2009). In

Published online: 17 July 2021

addition to these short-term (< 2 year) responses, the biological and chemical processes that ensue following disturbance can continue through the course of succession. For example, comparison of uptake in streams draining second growth (< 100 year) and old growth (> 400 year) forests suggests that stream uptake and watershed retention continue to increase over long successional timeframes (Valett et al., 2002). Thus, stream nutrient cycling responds to biological succession initiated by watershed disturbances.

In-stream hydrologic disturbances such as floods also influence nutrient uptake. High-discharge flood events prompt pulsed declines in reach-scale nutrient uptake due to enhanced downstream transport (e.g., spiral length increases with discharge; Ensign & Doyle 2006). As discharge returns to pre-flood conditions, uptake increases and spiral length contracts. However, floods also indirectly influence uptake by scouring stream biofilm communities. After discharge returns to pre-flood conditions, biofilm accrual and succession begin on bare substrates (Fisher et al., 1982; Ryder et al., 2006; Power et al., 2008). Benthic biofilms are a primary driver of stream nutrient demand (Mulholland et al., 1994; Webster et al., 2003), and consequently, flood-driven changes in biofilm succession could alter stream nutrient uptake after a hydrologic disturbance. Specifically, if a flood scours or buries benthic biofilms, once discharge returns to pre-flood conditions areal nutrient uptake should decline relative to pre-flood levels due to decreased biofilm biomass. However, flood pulses can also enhance floodplain connectivity, which promotes groundwater exchange and biological nutrient demand by microbes and plants in the riparian zone (Hall et al., 2009a; Harvey et al., 2019). After the flood, groundwater exchange continues to stimulate algae and heterotrophs growing on the channel benthos (Brookfield et al., 2021). In turn, as benthic succession progresses and biofilms accrue, areal uptake should increase.

Indeed, seminal research in Sycamore Creek (AZ, USA) demonstrates that in hydrologically flashy streams, uptake declines immediately following a flood, then quickly recovers with successional time as biofilms accrue (Fisher et al., 1982; Grimm, 1987; Martí et al., 1997). However, biofilm accrual and succession likely differ among streams and seasonal timeframes due to variation in nutrient supply (Biggs & Smith, 2002; Passy & Larson, 2011), groundwater exchange (Brookfield et al., 2021), light availability and temperature (Battin et al., 2016), and top-down controls (Mulholland et al., 1991). Sediment disturbances during or after flooding can also influence the recovery of biofilms and their nutrient demand throughout succession (Biggs et al., 1999; Gerull et al., 2012; Uehlinger & Naegeli, 1998). Thus, stream nutrient uptake is expected to increase with successional time following in-stream disturbances such as floods, but the rate of increase is likely to vary among systems or depend on the seasonal timing of the flood (Power et al., 2015).

Other than Sycamore Creek, there are few direct studies of how floods modulate stream nutrient demand or retention (but see Hanafi et al., 2006; von Schiller et al., 2008; Mueller Price et al., 2015). Here, we present two summers of uptake and biofilm measurements in the East River, a high elevation oligotrophic stream near the Rocky Mountain Biological Laboratory (RMBL) in the Elk Mountains of central Colorado, USA (Fig. 1). On 19 July 2017, a large rain event increased stream discharge by 340% relative to the previous week's average discharge, rising to within ~ 60% of the spring snowmelt peak maximum daily average discharge (Fig. 2). This rainfall event also caused a landslide on the southwest side of Bellview Mountain ~ 1 km downstream of Emerald Lake, the East River's origin (B. Taylor *personal observation*). The slide visually increased the turbidity ~ 61 km downstream to the confluence with the Taylor River (Reaman, 2017). The event deposited a ~ 1–3 mm layer of fine sediment into the East River that covered the benthos until at least October 2017. Other increases in discharge in 2017 resulted in smaller increases in discharge, ranging from 12 to 26% of the spring snowmelt peak). In 2018, the river did not experience any large midsummer floods (excursions ranged from 15 –40% of spring snowmelt peak) or geomorphic disturbance events similar to the 2017 landslide (Fig. 2), though rainfall-associated landslides and sediment deposition similar to the 2017 event are not uncommon. In the absence of midsummer disturbance (i.e., 2018), we expected that areal uptake would be greatest in the early spring after snowmelt floods receded due to high nutrient availability in meltwater (Corriveau et al., 2011; Williams & Melack, 1991) and rapid biofilm accrual on bare substrates. We then expected that areal uptake would

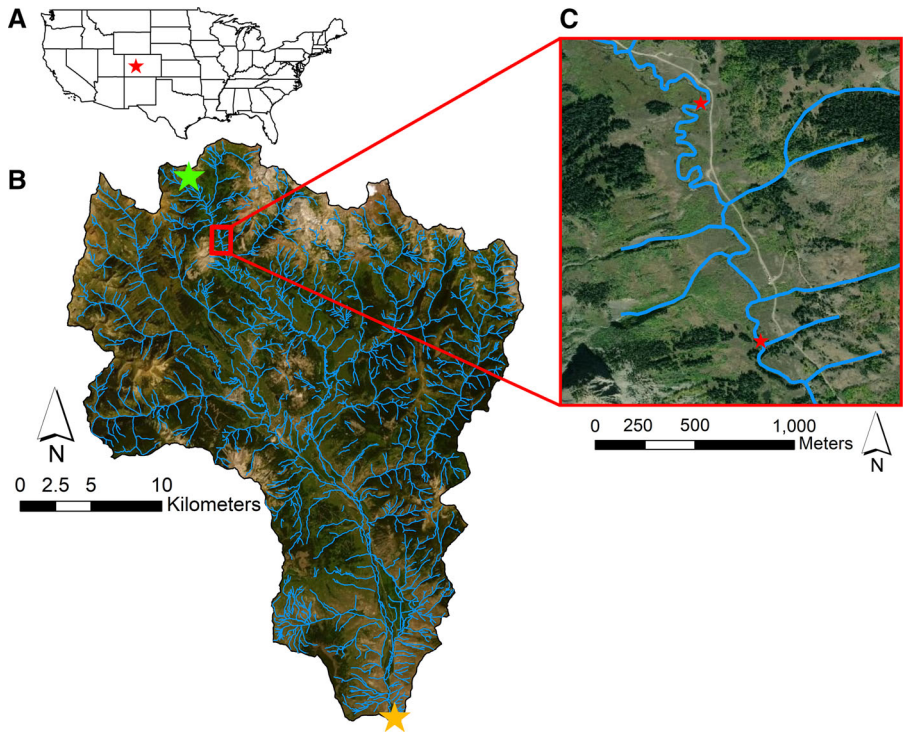

Fig. 1 **A** Location of the East River Watershed in Colorado, USA. **B** Delineation of the East River Watershed and satellite land imagery with a red box indicating the experimental reach. Green star indicates land slide origin on southwest side of Bellview Mountain. Orange star indicates reported visible downstream extent of sediment transport to the Gunnison River at the East-Taylor confluence near Almont, CO (Reaman 2017). **C** Upstream injection (38°58′26″N 106°59′49″W) and downstream (38°57′47″N 106°59′39″W) sampling location along the study reach, denoted by red stars. Three of the four tributary streams entering the delineated study reach section flow intermittently

decline over the summer as nutrient availability decreased and biofilms senesced and sloughed. We expected that the 2017 midsummer flood would disrupt this seasonal trajectory by scouring and burying benthic biofilms. Specifically, we expected that following the reset of successional processes by the midsummer flood, areal uptake would increase over the remainder of the summer.

Methods

Study site

The 2.475 km third-order reach along the East River has a contributing watershed area of 44.7 km^2. The reach begins below the inflow of Avery Creek and ends above the RMBL townsite (Fig. 1). Discharge was primarily snowmelt driven, with maximum daily mean snowmelt flows of 12.3 m^3/s in 2017 (26 May–27 June; Fig. 2) and 9.5 m^3/s in 2018 (3 May–16 June; Fig. 2). During these spring snowmelt intervals, total discharge was 1.94×10^7 m^3 in 2017 and 2.07×10^7 m^3 in 2018. Channel geomorphology includes a series of alternating riffles and pools along low gradient meanders with one intermittent side channel that typically flows through late July. The channel bed is primarily cobble with some stretches of bedrock, pebble, and sediment.

Stream stage and water temperatures were recorded continuously throughout both years with a Levelogger® model 3001-M5 datalogger (Solinst Canada Ltd, Georgetown, ON, Canada). Stage was used to predict discharge via a linear regression power function from measured discharge with a YSI Sontek Flowtracker (Xylem Inc, San Diego, CA, USA). Hourly mean photosynthetically active radiation (PAR) measurements were recorded by the RMBL weather station at Judd Falls, located 750 m from the downstream end of

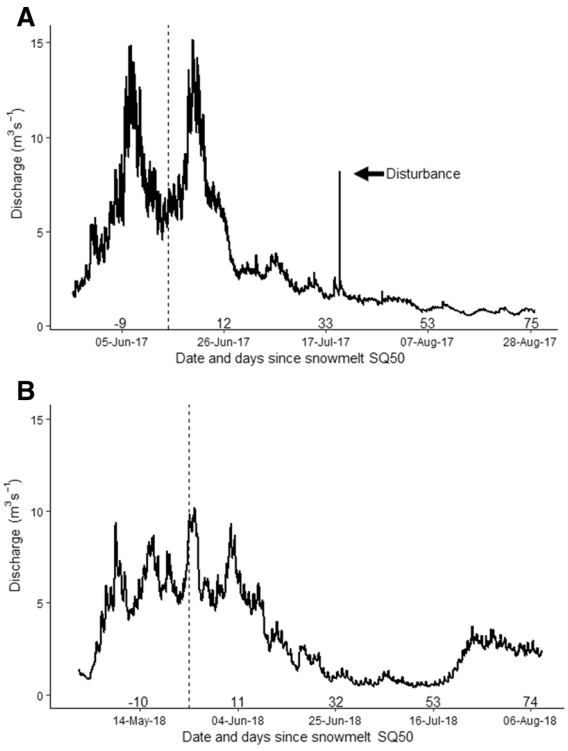

Fig. 2 Hydrographs for the East River in **A** 2017 and **B** 2018 at the study reach located above the Rocky Mountain Biological Laboratory. Dotted line denotes date of snowmelt SQ50 (14 June 2017 and 24 May 2018). X-axis labels above axis give days since date of snowmelt SQ50

the focal reach (Billick 2020; https://www.digitalrmbl.org/collections/weather-stations/).

To compare seasonal trajectories between years with different snowmelt timing, we developed a seasonal metric of snowmelt peakflow timing (SQ50) that is similar to the annual hydrograph center of mass (see Q50 in Clow 2010 or CT in Stewart et al., 2005) but differs in that it was calculated for a seasonal window of the hydrograph. First, we defined the snowmelt peak by visually identifying the initial date of the hydrograph rising limb in early spring and the final date of the descending limb in early summer (26 May–27 June 2017 and 3 May–16 June 2018; Fig. 2). Next, we used the pk.cov() function in the R package "FlowScreen" to calculate center of mass during these snowmelt peaks (hereafter Snowmelt Q50 or SQ50) (Dierauer & Whitfield, 2019). All sample dates were recoded as days since SQ50 for statistical analyses and comparison between years.

Nutrient Uptake Measurements

We measured reach-scale NH_4^+-N and PO_4^{3-}-P (as SRP) uptake six times from June through September during both summers using the Tracer Additions for Spiraling Curve Characterization (TASCC) method (Covino et al., 2010). For each nutrient uptake measurement, we added rhodamine water tracer (RWT, hydrologic tracer) and either ammonium chloride (NH_4Cl) or sodium phosphate (Na_2HPO_4) at the upstream reach endpoint. Our instantaneous injections raised downstream tracer and nutrient concentrations $\sim$ 10–20 $\times$ above ambient. We determined appropriate tracer and nutrient injectate masses by collecting ambient nutrient samples prior to each injection and estimating discharge at our experimental reach through a regression with a downstream USGS stream gauge (East River at Cement Creek, CO; USGS 09112200). During each nutrient release, we continuously monitored the RWT breakthrough curve (BTC) at the downstream reach endpoint with a Databank handheld fluorometer (Turner Designs, San Jose, CA, USA). Syringes fitted with inline filter holders containing Gelman AE glass fiber filters (Pall Gelman, Port Washington, NY, USA) were used to collect and filter 30–40 water samples for NH_4^+-N or PO_4^{3-}-P during each BTC. Following each BTC, $\sim$ 40 width measurements were collected along the reach and discharge was measured.

Nutrient samples were kept on ice until returning to the lab and were either analyzed immediately or refrigerated until analysis the following day. We measured NH_4^+-N using a standard fluorometric method established by Holmes et al. (1999) and modified by Taylor et al. (2007) on a Turner Designs Trilogy Fluorometer Model # 7200 (Sunnyvale, CA, USA). We measured SRP using conventional colorimetry (Murphy & Riley, 1962) on a Thermo Scientific GENESYS 10S UV–VIS Spectrophotometer (Waltham, MA, USA). Because ambient phosphorus concentrations in the East River typically fall near or below the detection limit of the conventional colorimetry (2.5 $\mu g\ L^{-1}$), ambient SRP samples were pre-concentrated 70-fold using Sargasso Sea water magnesium hydroxide co-precipitation (MAGIC-P; Anagnostou & Sherrell, 2008) and subsequently analyzed following conventional colorimetry. Our MAGIC-P protocol SRP detection limit was 0.04 $\mu g\ L^{-1}$. We also used the MAGIC-P pre-concentration

technique for the first and final three BTC samples because without pre-concentration they were typically near or below the detection limit of conventional colorimetry.

We calculated nutrient uptake via the TASCC method (Covino et al., 2010). Briefly, this method compares the ratio of added nutrient:tracer (i.e., NH_4^+-N or PO_4^{3-}-P; nutrient X:RWT) in each sample to the injectate ratio. For each sample across the BTC, we estimated added nutrient longitudinal uptake rate ($k_{w\text{-}add\text{-}X}$) as the slope of a two-point regression between stream distance and the natural logarithms of injectate and sample nutrient:tracer ratios (regression points one and two). The negative inverse of $k_{w\text{-}add\text{-}X}$ is the added nutrient uptake length ($S_{w\text{-}add\text{-}X}$) for each sample. Because ambient uptake length ($S_{w\text{-}amb\text{-}X}$) is sensitive to discharge, ambient areal uptake ($U_{amb\text{-}X}$) was used to compare nutrient demand over time. To estimate $U_{amb\text{-}X}$, $S_{w\text{-}add\text{-}X}$ was used to calculate areal uptake rates for each BTC sample ($U_{add\text{-}X}$) as:

$$U_{add-X} = \frac{Q \times [X_{add}]}{w \times S_{w-add-X}} \quad (1)$$

where Q is stream discharge, $[X_{add}]$ is the geometric mean of observed and conservative concentration of nutrient X, and w is average wetted channel width. We then estimated $U_{amb\text{-}X}$ for each nutrient release by regressing the BTC $U_{add\text{-}X}$ values against the geometric mean of observed and conservative nutrient concentrations (X_{add}) and extrapolating to ambient nutrient concentration at the Y intercept (Covino et al., 2010). Next, we estimated ambient uptake velocity ($V_{f\ amb\text{-}X}$) to assist in identifying important biotic and abiotic drivers of uptake because $U_{amb\text{-}X}$ can be highly correlated with ambient nutrient concentration. Specifically, $U_{add\text{-}X}$ was used to calculate uptake velocities for each BTC sample ($V_{f\ add\text{-}X}$) as:

$$V_{f\ add-X} = \frac{U_{add-X}}{[X_{add}]} \quad (2)$$

and $V_{f\ amb\text{-}X}$ was estimated in the same way as $U_{amb\text{-}X}$. Finally, the standard error of the intercept was used to estimate 95% confidence intervals for $U_{amb\text{-}X}$ and $V_{f\text{-}amb\text{-}X}$, hereafter referred to as U and V_f. Across all NH_4^+–N and PO_4^{3-}-P uptake measurements, mass of nutrient salt injected did not influence estimated V_f (Supplemental Fig. 1).

Benthic Algal Sampling

We sampled benthic biofilms (algae and organic matter) on natural rock substrates and on 5 × 10 cm unglazed ceramic tiles. Tiles were installed on 6 July 2017 and 20 June 2018 (22 and 27 days after snowmelt SQ50) to minimize tile loss during high flows. We sampled rock biofilm approximately bi-weekly starting before the first reach-scale uptake measurement in 2018, but in 2017 we began sampling rock algae approximately bi-weekly after the flood to monitor accrual after the midsummer flood.

Rock biofilms were sampled by scrubbing the top surface on each of 3–4 randomly selected softball-sized rocks (120 ± 70 cm^2) with a nylon Smoker's toothbrush (Wisdom, Haverhill, Suffolk). The total rock area used to generate the pooled biofilm slurry was estimated by photographing scrubbed rocks and calculating the top surface areas with ImageJ2 (Rueden et al., 2017). Tiles were scrubbed in the same way, and because all tiles had the same dimensions, total surface area was calculated using the number of tiles scrubbed (n = 3–7).

Subsamples of rock and tile biofilm slurries were used for chlorophyll-a analysis. Chlorophyll-a subsamples were transferred to 25 mm Pall AE filters (Port Washington, New York, USA) and frozen until analysis. Prior to analysis, samples were extracted in 3 mL $MgCO_3$ buffered 90% ethanol for 6–12 h. Concentration was measured with a Turner Designs Trilogy Fluorometer Model # 7200 (Sunnyvale, CA, USA) and converted to g m^{-2} following Steiman et al. (2017). After the chlorophyll subsample, the remaining rock and tile biofilm slurries were dried, weighed, ground and combusted at 500°C for two hours to determine ash-free dry mass (AFDM). Ash-free subsamples were then digested with $K_2S_2O_8$, diluted with deionized water, and analyzed for percent phosphorus content (% P) following standard colorimetry (Murphy & Riley, 1962; Ostrofsky & Rigler, 1987).

Statistical Analyses

All statistical analyses were performed in R 4.0.2 (R Core Team, 2018). Due to the uncertainty inherent in estimated parameters, for all tests using U or V_f as a response variable we used a resampling procedure to determine statistical significance. Specifically, each ANCOVA and linear model was run 1000 times with

different random values for each date's U and V_f selected from normal distributions with means equal to the date's average U or V_f and variance equal to the standard error of the date's average U or V_f. We report the percent of the 1000 statistical model iterations with $P \leq 0.05$ and $P \leq 0.1$ and considered terms significant when $\geq 95\%$ of $P \leq 0.1$.

First, to compare changes in U over time (trajectories) between 2017 and 2018, we used analysis of covariance (ANCOVA, model: U = Days since SQ50 + Year + Days since SQ50*Year). We used this approach to compare uptake trajectories between the two years across two timeframes; the "whole season" including all uptake measurements in both years, and after the timing of the 2017 midsummer flood and the same timeframe in 2018 (ANCOVA, model: U = 36 days after SQ50 + Year + 36 days after SQ50 *Year). For ANCOVAs with significant interaction terms, indicating the U trajectory differed between years, we used separate regressions to compare both years uptake trajectories to a null hypothesis of no change over time (linear model: U = Days since SQ50). We used a similar ANCOVA design to compare rock biofilm AFDM, Chl-a, and %P trajectories after day 36 between both years (model: Biofilm AFDM, Chl-a, or %P = 36 days after SQ50 + Year + 36 days after SQ50*Year), but there was no random sampling to evaluate uncertainty in these models because we do not have estimates of variability for biofilm parameters.

Next, to identify important biotic and abiotic drivers of uptake, we used both years uptake and biofilm measurements in separate linear models (biotic models: U or V_f = rock biofilm Chl-a to AFDM ratio + rock biofilm %P; abiotic models: U = Days since SQ50 + ambient nutrient concentration + average streamwater temperature during BTC + average PAR during BTC; abiotic V_f models excluded ambient nutrient concentration). We used the Chl-a to AFDM ratio (mg Chl-a per g AFDM) as a predictor term in biotic models because it is an index of living algal tissue relative to total biomass (e.g., Grimm & Fisher, 1986; Rosemond, 1993) and to conserve model degrees of freedom. We used analysis of variance (ANOVA) F tests to evaluate model terms for significance. Second, to compare the most important biotic and abiotic predictors of uptake, we built linear models of uptake that combined the biotic and abiotic terms that were significant in separate models (e.g., U = rock biofilm Chl-a to AFDM ratio + ambient nutrient concentration). Because biofilm samples were not always collected on the same days as NH_4^+-N and PO_4^{3-}-P uptake measurements (Figs. 3, 5), we used linear interpolation to estimate rock biofilm AFDM, chlorophyll, and %P contents on uptake sample dates that fell between biofilm samples. Finally, because biofilm sampling began midseason in 2017, we could not interpolate biofilm AFDM, chlorophyll, or %P for nutrient uptake measurements collected prior to day 45 (26 July 2017).

Results

Seasonal nutrient uptake trajectories

Across the season, NH_4^+-N U trajectories differed between 2017 and 2018 (interaction term, Table 1). In 2017, NH_4^+-N U did not change over the season (Fig. 3A; linear model: 0% of 1000 model iterations had $P \leq 0.1$). Whereas, in 2018 NH_4^+-N U declined by 98% across the season (Fig. 3A; linear model: 5% $P \leq 0.05$, 97% $P \leq 0.1$). PO_4^{3-}-P U trajectories across the season did not differ between 2017 and 2018 (no significant interaction term, Table 1). On average, PO_4^{3-}-P U declined by 91% across the season (Fig. 3B; Days since SQ50, Table 1).

When U is normalized by ambient nutrient concentrations (Fig. 4), NH_4^+-N and PO_4^{3-}-P V_f followed similar trajectories across the 2017 and 2018 seasons (No significant interaction terms; Table 1). On average, NH_4^+-N V_f declined by 84% across the season (Fig. 3C; Days since SQ50, Table 1). Likewise, PO_4^{3-}-P V_f declined by 74% across the season (Fig. 3D; Days since SQ50, Table 1).

Post disturbance nutrient uptake trajectories

After the 2017 midsummer flood (day 36) NH_4^+-N U trajectory over the remainder of the season did not differ between 2017 and the same timeframe in 2018 (no significant interaction term, Table 1). NH_4^+-N U did not change over time after day 36 in either year (Fig. 3A; no significant days after SQ50 term, Table 1). PO_4^{3-}-P U trajectories after day 36 differed between 2017 and 2018 (significant interaction term, Table 1). In 2017, PO_4^{3-}-P U after day 36 trended toward a 55% increase over time (Fig. 3B; 18%

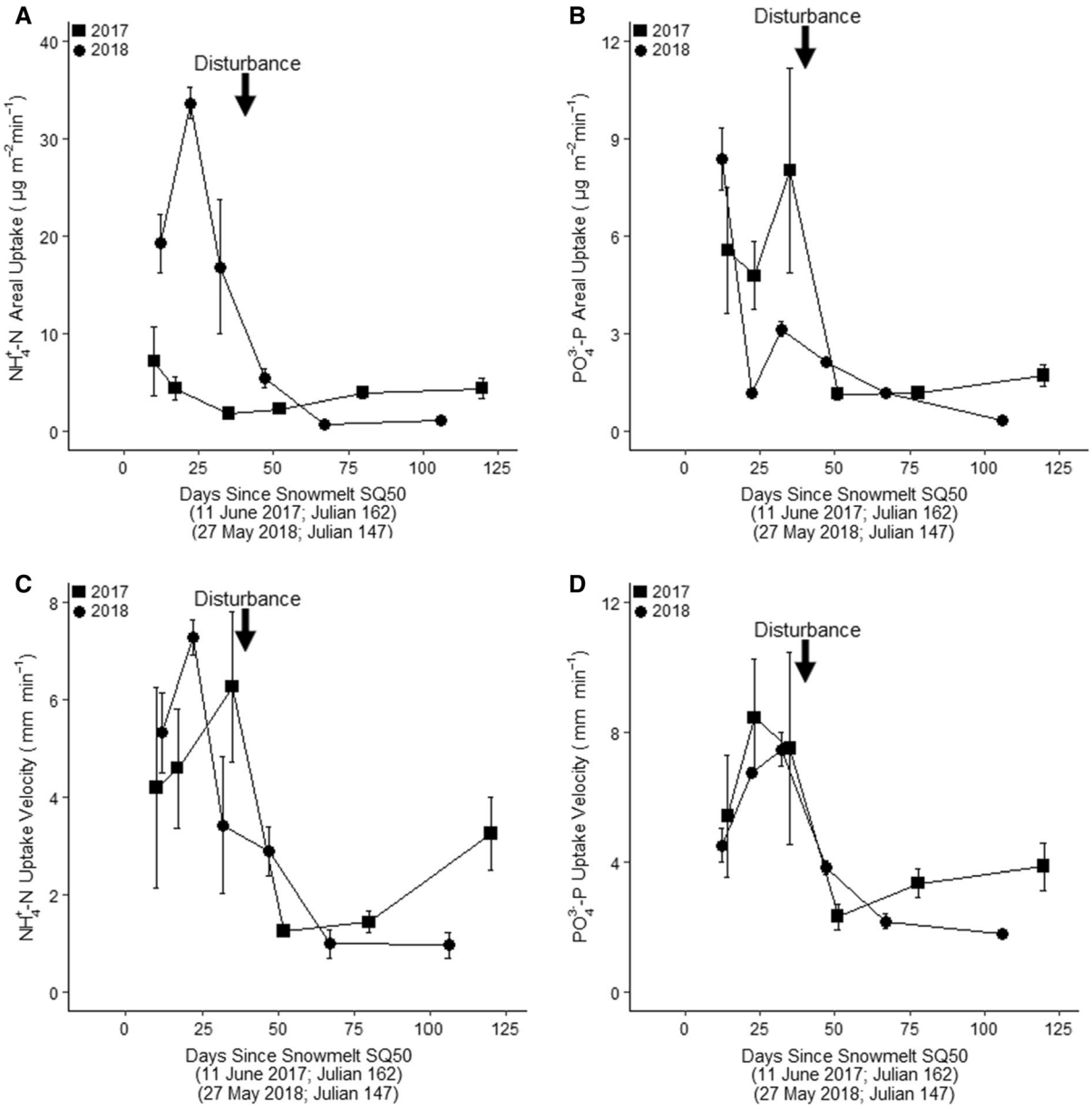

Fig. 3 2017 (square) and 2018 (circle) seasonal trajectories of ammonium (**A**) and phosphorus (**B**) areal uptake (*U*), as well as corresponding uptake velocities (V_f, **C** and **D**). Error bars represent 95% confidence intervals. A landslide occurred 19 July 2017 (36 days after snowmelt SQ50; denoted by arrow)

$P \leq 0.05$, 47% $P \leq 0.1$). Whereas, in 2018 PO_4^{3-}-P *U* after day 36 declined by 84% over time (Fig. 3B; 9% $P \leq 0.05$, 98% $P \leq 0.1$).

After day 36, NH_4^+-N V_f trajectories did not differ between 2017 and 2018 (No significant interaction term; Table 1), and did not change over the remainder of the season (Fig. 3C; No significant days since SQ50 term; Table 1). In contrast, PO_4^{3-}-P V_f trajectories after day 36 trended towards a difference between 2017 and 2018 (Fig. 3D; days since SQ50, Table 1). In 2017, PO_4^{3-}-P V_f after day 36 trended toward a 66% increase over time (Fig. 3D; 27% $P \leq 0.05$, 54% $P \leq 0.1$). Whereas, in 2018 PO_4^{3-}-P V_f after day 36 trended toward a 54% decline over time (Fig. 3D; 13% $P \leq 0.05$, 74% $P \leq 0.1$).

Table 1 Summary of ANCOVAs comparing changes in U and V_f over time between 2017 and 2018 (model: Uptake = Days since SQ50 + Year + Days since SQ50*Year)

Timeframe	Response	% of ANCOVAs where term $P \leq 0.05$			% of ANCOVAs where term $P \leq 0.1$		
		Days since SQ50	Year	Interaction	Days since SQ50	Year	Interaction
Whole season	NH_4^+-N U	77.1	24.0	86.6	**100.0**	87.1	**100.0**
	NH_4^+-N V_f	73.6	0	0	**97.1**	0	0.2
	PO_4^{3-}-P U	77.0	0	0	**99.2**	0	0
	PO_4^{3-}-P V_f	68.8	0	0	**97.4**	0	0
After day 36	NH_4^+-N U	0	0	0	0	0	0
(Date of 2017 midsummer flood)	NH_4^+-N V_f	0	0	0	0	0	10.3
	PO_4^{3-}-P U	1.5	0	89.4	11.4	0	**100.0**
	PO_4^{3-}-P V_f	0	0	0.5	0	0	47.0

For each of 1000 iterations of the ANCOVAs, random values were drawn for each dates' U and V_f from normal distributions with means equal to the date's average U or V_f and variance equal to the standard error of the date's average U or V_f. The percent of the 1000 ANCOVA iterations with $P \leq 0.05$ and $P \leq 0.1$ for each effect are reported below, with frequencies interpreted as significant in bold. This approach was used to compare changes in uptake over time between the two years across the whole season and for just the time interval after the date of the 2017 midsummer flood (36 days after SQ50). For the whole season timeframe, df = (1,8) for all effects, whereas for the time interval after the date of the 2017 landslide, df = (1,2)

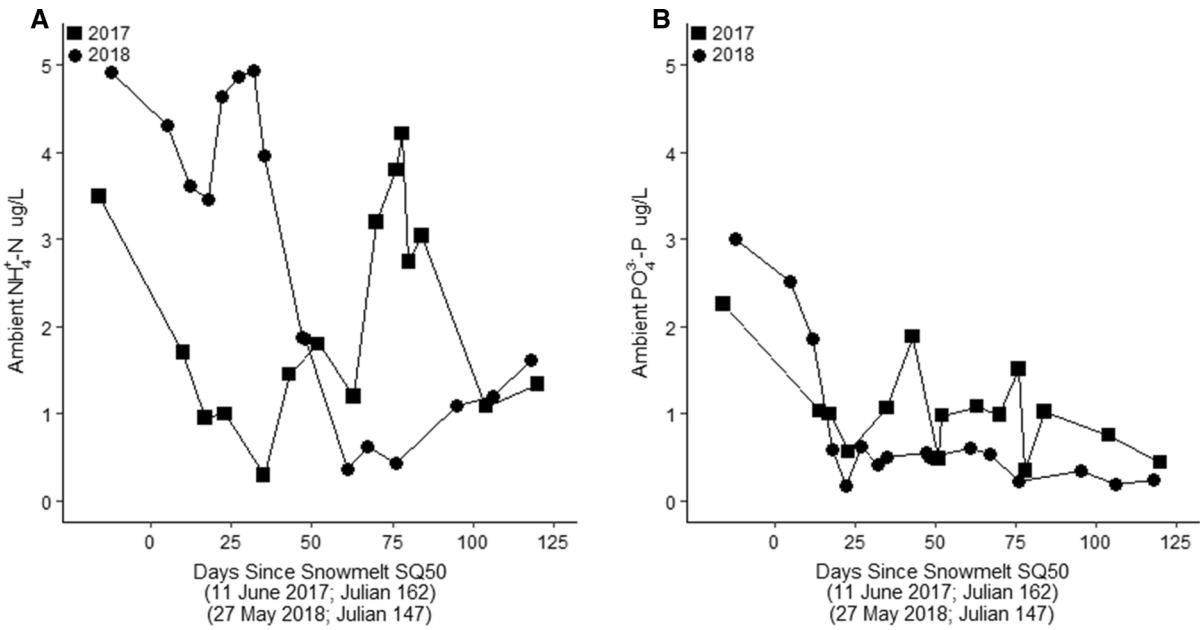

Fig. 4 East River ambient A) NH_4^+-N and B) PO_4^{3-}-P concentrations in 2017 (squares) and 2018 (circles). A landslide occurred 19 July 2017 (36 days after snowmelt SQ50; denoted by arrow)

Biofilms trajectories after the midsummer flood

After day 36, rock biofilm AFDM trajectories differed between 2017 and 2018 (ANCOVA interaction, Post 36 days*Year: $F_{1,5} = 12.03$, $P = 0.018$). In 2017, rock biofilm increased by 180% after the midsummer flood over the remainder of the growing season (Fig. 5A; $F_{1,2} = 28.15$, $P = 0.034$). Whereas, in 2018 rock biofilm AFDM declined by 79% over the entire growing season (Fig. 5A; $F_{1,3} = 11.93$, $P = 0.04$). Rock biofilm Chl-a, Chl-a per AFDM, and % P trajectories in 2017 and 2018 were

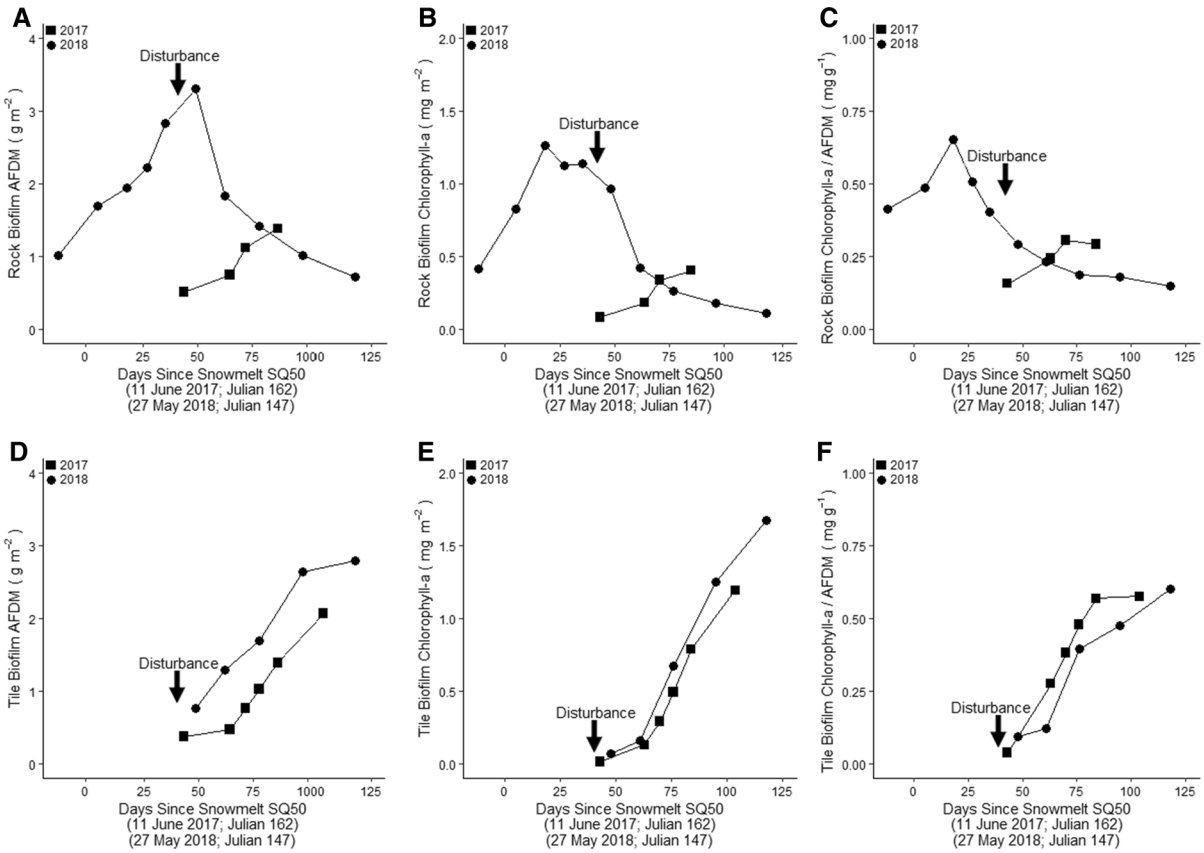

Fig. 5 2017 (square) and 2018 (circle) seasonal trajectories of biofilm AFDM (g m^{-2}), chlorophyll-a (mg m^{-2}), and chlorophyll-a to AFDM ratios (mg g^{-1}) on natural rock substrates (**A–C**) and on installed tiles (**D–F**). A landslide occurred 19 July 2017 (36 days after snowmelt SQ50; denoted by arrow)

directionally consistent with those of biofilm AFDM. Specifically, each biofilm parameter's trajectory after day 36 differed between 2017 and 2018 (ANCOVA interaction, Chl-a, Post 36 days*Year: $F_{1,5} = 9.05$, $P = 0.03$; Chl-a per AFDM, Post 36 days*Year: $F_{1,5} = 26.04$, $P < 0.001$; % P, Post 36 days*Year: $F_{1,5} = 25.4$, $P < 0.001$). In 2017, all biofilm parameters increased over time; Chl-a by 100% (Fig. 5B; $F_{1,2} = 22.98$, $P = 0.04$), Chl-a per AFDM by 88% (Fig. 5C; $F_{1,2} = 10.12$, $P = 0.08$), and % P by 150% (Fig. 5A; $F_{1,2} = 9.14$, $P = 0.09$). Whereas, in 2018, all biofilm parameters declined over time; Chl-a by 90% (Fig. 5B; $F_{1,3} = 7.99$, $P = 0.06$), Chl-a per AFDM by 52% (Fig. 5C; $F_{1,3} = 19.4$, $P = 0.02$), and % P by 45% (Fig. 6A; $F_{1,3} = 36.1$, $P < 0.01$).

In contrast to biofilms on natural rock substrates, biofilms on installed tiles had similar trajectories for all parameters in 2017 and 2018 (ANCOVA interaction, AFDM, post 36 days*Year: $F_{1,7} = 0.14$, $P = 0.91$; Chl-a, Post 36 days*Year: $F_{1,7} = 1.23$, $P = 0.31$; Chl-a per AFDM, Post 36 days*Year: $F_{1,7} = 0.61$, $P = 0.46$; % P, Post 36 days*Year: $F_{1,7} = 3.96$, $P = 0.11$). Specifically, all tile biofilm parameters increased over time in both years; AFDM by 600% on average (Fig. 5D; post 36 days: $F_{1,7} = 111.26$, $P < 0.001$), Chl-a by 16,000% (Fig. 5E; post 36 days: $F_{1,7} = 176.94$, $P < 0.001$), Chl-a per AFDM by 1400% (Fig. 5F; post 36 days: $F_{1,7} = 59.64$, $P < 0.001$), and % P by 100% (Fig. 6B; post 36 days: $F_{1,7} = 31.28$, $P < 0.001$).

Biotic and abiotic drivers of nutrient Uptake

Linear models with separate biotic and abiotic predictors suggest that NH_4^+-N and PO_4^{3-}-P uptake have similar drivers. Specifically, both nutrients' U and V_f increased with rock biofilm Chl-a to AFDM ratio (biotic-only models, Table 2). Both nutrient's

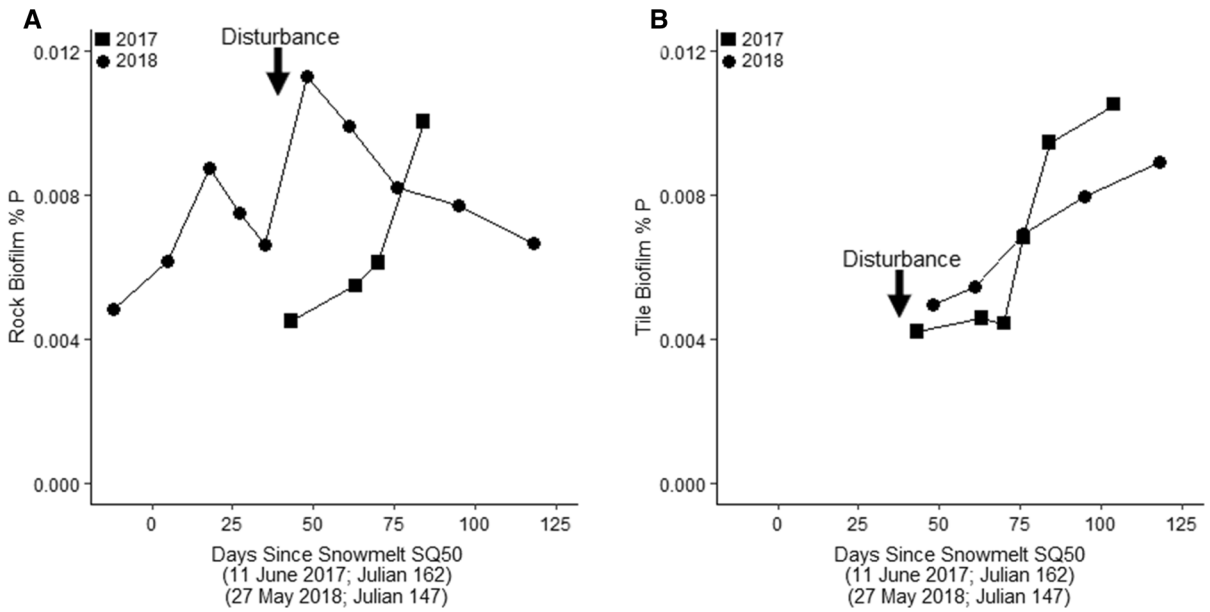

Fig. 6 2017 (square) and 2018 (circle) seasonal trajectories of biofilm percent phosphorus on natural rock substrates (**A**) and installed tiles (**B**). A landslide occurred 19 July 2017 (36 days after snowmelt SQ50; denoted by arrow)

U was greater at higher ambient nutrient concentrations, whereas their V_f declined with days since SQ50 (abiotic-only models, Table 2). When these 'best' biotic and abiotic predictors were included as predictors in the same models, rock biofilm Chl-a to AFDM ratio was the only significant predictor of V_f for both nutrients, and of NH_4^+-N *U* (Table 2). Whereas, both rock biofilm Chl-a to AFDM ratio and ambient PO_4^{3-}-P concentration were significant predictors of PO_4^{3-}-P *U* (Table 2).

Discussion

Here, we explored how a midsummer flood event influenced the seasonal trajectory of nutrient uptake in a montane stream that typically experiences a snowmelt-driven spring flood followed by relatively stable summer flows but occasional summer rainstorm-driven floods. Under relatively stable summer flow conditions in 2018, we found that both PO_4^{3-}-P and NH_4^+-N *U* were greatest in the early spring when benthic biofilms were accruing rapidly, then declined over the season as biofilms senesced. We expected that a midsummer flood event would alter this trajectory by scouring biofilms and subsequently prompting new accrual that would increase nutrient demand. Indeed, biofilms accrued after the 2017 midsummer flood, but because we did not sample biofilms before the flood event it is unclear if this accrual was re-initiated. Regardless, rock biofilm biomass declined during the same timeframe in 2018, suggesting that the 2017 midsummer flood altered the typical seasonal trajectory of benthic biofilms in the East River. In turn, PO_4^{3-}-P *U* increased after the 2017 midsummer flood, whereas it declined throughout the same timeframe during 2018. PO_4^{3-}-P V_f followed the same patterns as *U* during both timeframes in both years, suggesting that the increase in *U* after the 2017 midsummer flood was not driven by ambient nutrient concentrations alone. In contrast to PO_4^{3-}-P, NH_4^+-N *U* did not change after the 2017 midsummer flood, although it also did not decline across the whole season as it did in 2018. It is possible that NH_4^+-N demand increased after the 2017 midsummer flood, but only enough to preclude a late season decline in *U* similar to that observed in 2018. Visually, NH_4^+-N V_f does appear to increase in late 2017, although this change is not statistically significant. Thus, the 2017 midsummer flood altered the seasonal trajectory of PO_4^{3-}-P uptake, and possibly NH_4^+-N uptake as well.

Table 2 Summary of linear models with biotic only, abiotic only, and both biotic and abiotic predictors of uptake

Types of terms included	Linear model			% of models where term		
	Response	Predictor(s)	df (N,D)	$P \leq 0.05$	$P \leq 0.1$	Adj. R^2
Models of NH_4^+-N uptake						
Biotic only	NH_4^+-N U	Rock biofilm Chl-a/AFDM ratio	(1,6)	**100.0**	**100.0**	0.84
		Rock biofilm % P	(1,6)	0.0	0.0	
	NH_4^+-N V_f	Rock biofilm Chl-a/AFDM ratio	(1,6)	**100.0**	**100.0**	0.84
		Rock biofilm % P	(1,6)	0.0	0.0	
Abiotic only	NH_4^+-N U	Days since SQ50	(1,7)	0.0	0.0	0.75
		Ambient NH_4^+-N μg L^{-1}	(1,7)	**98.8**	**100.0**	
		Streamwater temperature °C	(1,7)	0.0	0.0	
		PAR	(1,7)	0.0	0.0	
	NH_4^+-N V_f	Days since SQ50	(1,8)	16.2	71.6	0.47
		Streamwater temperature °C	(1,8)	0.3	0.31	
		PAR	(1,8)	0.1	0.2	
Best biotic and abiotic	NH_4^+-N U	Rock biofilm Chl-a/AFDM ratio	(1,6)	**65.0**	**96.4**	0.86
		Ambient NH_4^+-N μg L^{-1}	(1,6)	0.0	0.9	
	NH_4^+-N V_f	Rock biofilm Chl-a/AFDM ratio	(1,6)	**100.0**	**100.0**	0.87
		Days since SQ50	(1,6)	0.0	1.7	
Models of PO_4^{3-}-P uptake						
Biotic only	PO_4^{3-}-P U	Rock biofilm Chl-a/AFDM ratio	(1,6)	0.0	**100.0**	0.45
		Rock biofilm % P	(1,6)	0.0	0.0	
	PO_4^{3-}-P V_f	Rock biofilm Chl-a/AFDM ratio	(1,6)	**100.0**	**100.0**	0.68
		Rock biofilm % P	(1,6)	0.0	0.0	
Abiotic only	PO_4^{3-}-P U	Days since SQ50	(1,7)	1.1	9.3	0.82
		Ambient PO_4^{3-}-P μg L^{-1}	(1,7)	**99.6**	**100.0**	
		Streamwater temperature °C	(1,7)	0.0	1.5	
		PAR	(1,7)	0.0	0.0	
	PO_4^{3-}-P V_f	Days since SQ50	(1,8)	30.9	87.6	0.45
		Streamwater temperature °C	(1,8)	0.0	0.1	
		PAR	(1,8)	0.0	0.0	
Best biotic and abiotic	PO_4^{3-}-P U	Rock biofilm Chl-a/AFDM ratio	(1,6)	**100.0**	**100.0**	0.96
		Ambient PO_4^{3-}-P μg L^{-1}	(1,6)	**100.0**	**100.0**	
	PO_4^{3-}-P V_f	Rock biofilm Chl-a/AFDM ratio	(1,6)	68.4	**99.7**	0.68
		Days since SQ50	(1,6)	0.0	0.0	

For each of 1000 iterations of the linear models, random values were drawn for each dates' U and V_f from normal distributions with means equal to the date's average U or V_f and variance equal to the standard error of the date's average U or V_f. The percent of the 1000 model iterations with $P \leq 0.05$ and $P \leq 0.1$ for each term are reported below, with frequencies interpreted as significant in bold. Interaction terms were not included in models. For "df", N = numerator, D = denominator

Installed tiles suggest midsummer accrual is constrained in established biofilms

In contrast to biofilm accrual on rock substrates after the 2017 midsummer flood, biomass (AFDM and chlorophyll) declined during the same timeframe in 2018. However, accrual on installed tile substrates in both years was similar to accrual on flood-disturbed rock substrates in 2017. The contrasting trajectories of tile and rock biofilms in 2018 demonstrates that the

river had capacity for accrual on bare surfaces midsummer, but not on rocks with established biofilms. Interestingly, this suggests that historical successional effects, competition, or midsummer environmental conditions such as water temperature, light, or nutrient availability may have constrained accrual and prompted community turnover or senescence and sloughing in established biofilms, but not on midsummer flood-disturbed rocks (2017) or bare tiles (2017 and 2018).

For example, temperature could constrain accrual or prompt community shifts in established biofilms because the East River warms over the season (e.g., Supplemental Fig. 2). Although diatoms are typically among the first to colonize stream benthos, they perform best at low temperatures and high nutrients (DeNicola, 1996; Fisher et al., 1982) and may senesce and slough at higher temperatures (Diaz Villanueva et al., 2011). Alternatively, ambient NH_4^+-N concentrations after the 2017 midsummer flood were high relative to the same period in 2018, but PO_4^{3-}-P concentrations were low in both years (Fig. 4). Non-overlapping NH_4^+-N and PO_4^{3-}-P V_f 95% confidence intervals on 2/3 dates during this timeframe in 2017 and 3/3 dates in 2018 suggest that when uptake is normalized to ambient supply, demand for PO_4^{3-}-P is generally greater than demand for NH_4^+-N. This pattern is consistent with the P limitation or co-limitation measured with nutrient diffusing substrate biomass responses in the East River and other nearby streams (Fuller & Peckarsky, 2011; Taylor *unpublished data*). Therefore, P-limitation could constrain biofilm accrual or maintenance.

Uptake increases with proportion of algal tissue in biofilms

The proportion of rock biofilm Chl-a per AFDM was a consistent predictor of NH_4^+-N and PO_4^{3-}-P U and V_f. Specifically, across all of summer 2018 and the timeframe of 2017 for which we have biofilm measurements, greater proportions of Chl-a per AFDM were associated with greater uptake, suggesting that living algal tissue is an important driver of nutrient uptake in the East River, as has been demonstrated elsewhere (Docherty et al., 2018; Martí et al., 1997; Mulholland et al., 1994). Surprisingly, biofilm % P was not linked to uptake of either nutrient despite likely P-limitation (Fuller & Peckarsky, 2011; Taylor *unpublished data*). This may be because SRP concentrations were consistently very low across the two summers (e.g., 2–3 µg/L near SQ50, generally < 1 µg/L thereafter) and others report consistent seasonal declines downstream of the study reach (Arora et al., 2020). Thus, in oligotrophic streams, nutrient uptake may be more closely linked to biofilm quantity than stoichiometric quality.

Among the abiotic drivers of uptake we considered, the importance of time since SQ50 as a predictor of both NH_4^+-N and PO_4^{3-}-P uptake velocities suggests that seasonal processes exert important controls on demand in the East River. During snowmelt in montane streams, enhanced floodplain connectivity promotes increased nutrient demand by microbes and plants in the riparian zone (Hall et al., 2009a). Our uptake estimates via the TASCC method cannot directly quantify demand in the hyporheic or riparian like the 15N isotope tracer used by Hall et al. (2009b), but our measurements represent the sum of nutrient demand across all reactive compartments. Thus, enhanced hyporheic and riparian connectivity during the early season complements high early season biofilm nutrient demand to explain the consistent high early season NH_4^+-N and PO_4^{3-}-P uptake observed in 2017 and 2018.

Decline in ambient nutrient supply was the most important abiotic seasonal process that contributed to declines in areal uptake across the season. Indeed, ambient supplies alone explained large amounts of seasonal variation in areal uptake (75–82%) and considering biofilm AFDM as well yielded only modest improvements (86–96%). In streams with snowmelt-driven hydrology, this predictable ambient supply decline occurs as snowpacks melt and release stored nutrients (Corriveau et al., 2011; Williams and Melack, 1991). Thus, the importance of time since SQ50 as a predictor of both nutrients' uptake likely reflects the seasonal decline in ambient nutrient concentration after SQ50.

Surprisingly, average water temperature during uptake measurements did not predict NH_4^+-N or PO_4^{3-}-P uptake. Warmer temperatures should increase nutrient demand by accelerating microbial metabolism (Diaz Villanueva et al., 2011; Yvon-Durocher et al., 2010) and the kinetics of sediment adsorption (Zhang & Huang, 2011). Nutrient uptake measurements in the East River spanned temperatures from 4°C to 15°C, within the range that some studies

detect temperature driven differences in uptake (Coble et al., 2019; Williamson et al., 2016). However, an important distinction between those studies and this study is that they report temperature gradients across streams or seasons, whereas this study is within the same system in the same season. Thus, temperature effects in other studies may be representative of biofilm communities that developed under distinctly different thermal regimes rather than temperature-driven variation in uptake kinetics. The inter-biome LINX study provides some precedent for the absence of temperature-driven influence on uptake (Webster et al., 2003). Alternatively, the effect size of temperature over the 10° range we sampled may just be small relative to the importance of other drivers.

Light availability also did not predict uptake of either nutrient despite nearly 46-fold variation in PAR among uptake measurements. Light availability can enhance microbial N uptake and transformations in streams (Hall et al., 2009b; Mulholland et al., 2006) and is generally expected to stimulate photosynthesis or increase photosynthetic rates (Gu & Wyatt, 2016). Importantly, our PAR measurements were not collected in situ, and therefore we cannot detect how surrounding topography, water depth, and turbidity mediate light availability at the benthos (Julian et al., 2008). However, variation in canopy cover is not a concern with using these PAR measurements because this reach of the East River as well as several km upstream and downstream has little to no deciduous tree canopy cover. With these caveats in mind, the apparent unimportance of light availability on East River nutrient uptake suggests that autotrophic components of biofilms may have less influence on uptake than the heterotrophs, which may be limited by nutrient availability rather than constrained by temperature. Thus, as snowpack nutrients are depleted over the season and flow declines, groundwater exchange may become increasingly important to benthic biofilms (Brookfield et al., 2021). Indeed, groundwater exchange may be critical for benthic biofilms throughout the season, as high transfer of dissolved organic carbon from East River floodplain soils during snowmelt (Winnick et al., 2017) may promote primarily heterotrophic biofilm development by releasing nascent heterotrophs from dependence on algal carbon exudates (Diaz Villanueva et al., 2011).

Besides the drivers of uptake we explored and the likely importance of groundwater interactions, there are several additional mechanisms we were not able to test. First, total uptake estimated by the TASCC method does not discriminate between assimilatory uptake and adsorption to sediments. Greater suspended sediment loads during the high discharge phases of the early summer could enhance physical adsorption and contribute to the faster uptake observed early in the season (Blanco et al., 2010). Sediment adsorption is classically recognized as a mechanism for binding P but NH_4^+-N can also bind to sediments (Triska et al., 1994). Additionally, from a landscape perspective this abiotic uptake mechanism does not necessarily result in the same nutrient retention as assimilatory uptake that binds nutrients in place because nutrients bound to sediment particles can still be transported downstream (D'Angelo et al., 1991). Therefore, if adsorption makes large contributions to reach-scale uptake at any point in the season, the seasonal trajectory of uptake may not reflect that of retention.

Second, rates of production and respiration provided by estimates of stream metabolism should correlate more closely with assimilatory uptake than the standing stocks we measured (Hall & Tank, 2003; Covino et al., 2018). Indeed, stream metabolism and primary productivity should be most sensitive to nutrient availability in oligotrophic streams (Bernhardt et al., 2018) such as the East River, and by extension their uptake kinetics should also be most sensitive to rapid changes in benthic biofilms (Bothwell, 1989). Although biofilm biomass and chlorophyll standing stocks generally correlate with gross primary production (Biggs et al., 1999), the ability of standing stocks to explain variation in uptake may be limited relative to direct measures of metabolism because we only measured biofilms on rocks and installed tiles. Biofilms growing on different substrates can have different nutrient requirements (Hanrahan et al., 2018). Fine sediments are abundant in the East River, and it is likely that the surface areas of fine sediment versus rock streambed are not equal. Additionally, we purposely selected moderately-sized rocks, which may have further limited our ability to characterize reach-scale biofilms. Therefore, although the proportion of living algal tissue in rock biofilms control uptake in the East River, our biofilm measurements are an imperfect index of assimilatory demand.

In streams that flood frequently, such as Sycamore Creek, nutrient uptake sharply declines immediately

after a flood, then gradually increases as biofilm biomass accumulates (Fisher et al., 1982). However, biofilm accrual and succession likely differ among streams due to variation in biotic and abiotic conditions, and furthermore the extent to which biofilm biomass drives uptake could vary among systems. We show that, in a stream that infrequently receives floods during the growing season, biofilm accrual following a midsummer flood is a significant predictor of nutrient processing rates. More studies exploring how floods affect nutrient uptake are needed to identify generalities and system-specific responses as well as the importance of historical constraints imposed by predictable flood events, such as snowmelt floods, on biofilm community development and nutrient uptake.

Acknowledgments We thank the Rocky Mountain Biological Laboratory for research approval and logistic support. We thank E. Binck, B. Swift, J. Fitzgerald, J. Forbes, E. Jameson, and N. Taylor for field assistance. Comments from two anonymous reviewers, M. Demi and S. Jordt improved the manuscript. Balik was supported by an NSF Graduate Research Fellowship, a Southeast Climate Adaptation Science Center Global Change Fellowship, a Colorado Mountain Club Foundation Al Ossinger Fellowship, and a RMBL Graduate Fellowship. Additional funding was provided by NSF IOS 1641041, NSF DEB 1556914, and North Carolina State University to B. Taylor.

Funding Balik was supported by an NSF Graduate Research Fellowship, a Southeast Climate Adaptation Science Center Global Change Fellowship, a Colorado Mountain Club Foundation Al Ossinger Fellowship, and a RMBL Graduate Fellowship. Additional funding was provided by NSF IOS 1641041, NSF DEB 1556914, and North Carolina State University to B. Taylor.

Availability of data and material Data available upon request.

Declarations

Conflict of interest The authors declare that they have no conflict of interest.

References

Anagnostou, E. & R. M. Sherrell, 2008. MAGIC method for subnanomolar orthophosphate determination in freshwater. Limnology and Oceanography: Methods 6: 64–74.

Arora, B., M. Burrus, M. Newcomer, C. I. Steefel, R. W. Carroll, D. Dwivedi, W. Dong, K. H. Williams & S. S. Hubbard, 2020. Differential CQ Analysis: a new approach to inferring lateral transport and hydrologic transients within multiple reaches of a mountainous headwater catchment. Frontiers in Water 2: 2–24.

Battin, T. J., K. Besemer, M. M. Bengtsson, A. M. Romani & A. I. Packmann, 2016. The ecology and biogeochemistry of stream biofilms. Nature Reviews Microbiology 14: 251–263.

Bernhardt, E. S., G. E. Likens, D. C. Buso & C. T. Driscoll, 2003. In-stream uptake dampens effects of major forest disturbance on watershed nitrogen export. Proceedings of the National Academy of Sciences 100: 10304–10308.

Bernhardt, E. S., J. B. Heffernan, N. B. Grimm, E. H. Stanley, J. W. Harvey, M. Arroita, A. P. Appling, M. J. Cohen, W. H. McDowell, R. O. Hall Jr., J. S. Read, B. J. Roberts, E. G. Stets & C. B. Yackulic, 2018. The metabolic regimes of flowing waters. Limnology and Oceanography 63: S99–S118.

Biggs, B. J. F. & R. A. Smith, 2002. Taxonomic richness of stream benthic algae: effects of flood disturbance and nutrients. Limnology and Oceanography 47: 1175–1186.

Biggs, B. J. F., R. A. Smith & M. J. Duncan, 1999. Velocity and sediment disturbance of periphyton in headwater streams: biomass and metabolism. Journal of the North American Benthological Society 18: 222–241.

Billick, 2020. Installation, maintenance and publication of data from the RMBL weather stations has been supported by NSF award (MRI0821369), NSF Grant DBI #0821369, and DOE funding as well as ongoing operational support from RMBL, the upper Gunnison River Water Conservancy District and the LBNL science focus area 2.0 project. https://www.digitalrmbl.org/collections/weather-stations/. Accessed 17 January 2020.

Blanco, A. C., K. Nadaoka, T. Yamamoto & K. Kinjo, 2010. Dynamic evolution of nutrient discharge under stormflow and baseflow conditions in a coastal agricultural watershed in Ishigaki Island, Okinawa, Japan. Hydrological Processes 24: 2601–2616.

Bothwell, M. L., 1989. Phosphorus–limited growth dynamics of lotic periphytic diatom communities: areal biomass and cellular growth rate responses. Canadian Journal of Fisheries and Aquatic Sciences 46: 1293–1301.

Brookfield, A. E., A. T. Hansen, P. L. Sullivan, J. A. Czuba, M. F. Kirk, L. Li, M. E. Newcomer & G. Wilkinson, 2021. Predicting algal blooms: are we overlooking groundwater? Science of The Total Environment 769: 1–15.

Clow, D. W., 2010. Changes in the timing of snowmelt and streamflow in Colorado: a response to recent warming. Journal of Climate 23: 2293–2306. https://doi.org/10.1175/2009jcli2951.1

Coble, A. A., A. M. Marcarelli & E. S. Kane, 2019. Year-round measurements reveal seasonal drivers of nutrient uptake in a snowmelt-driven headwater stream. Freshwater Science 38: 156–169.

Corriveau, J., P. A. Chambers, A. G. Yates & J. M. Culp, 2011. Snowmelt and its role in the hydrologic and nutrient budgets of prairie streams. Water Science Technology 64: 1590–1596.

Covino, T. P., B. L. McGlynn & R. A. McNamara, 2010. Tracer Additions for Spiraling Curve Characterization (TASCC): quantifying stream nutrient uptake kinetics from ambient to saturation. Limnology and Oceanography: Methods 8: 484–498.

Covino, T. P., E. S. Bernhardt & J. B. Heffernan, 2018. Measuring and interpreting relationships between nutrient supply, demand, and limitation. Freshwater Science 37: 448–455.

D'Angelo, D. J., J. R. Webster & E. F. Benfield, 1991. Mechanisms of stream phosphorus retention: an experimental study. Journal of the North American Benthological Society 10: 225–237.

DeNicola, D. M., 1996. Periphyton responses to temperature at different ecological levels. In Stevenson, R. J., M. L. Bothwell & R. L. Lowe (eds.), Algal Ecology: Freshwater Benthic Ecosystems. Academic Press, San Diego, California: 149–181.

Diaz Villanueva, V., J. Font, T. Schwartz & A. M. Romani, 2011. Biofilm formation at warming temperature: acceleration of microbial colonization and microbial interactive effects. Biofouling 27: 59–71.

Dierauer, J. & P. Whitfield, 2019. FlowScreen: Daily Streamflow Trend and Change Point Screening. R package version 1.2.6. https://CRAN.R-project.org/package=FlowScreen

Docherty, C. L., T. Riis, D. M. Hannah, S. Rosenhøj Leth & A. M. Milner, 2018. Nutrient uptake controls and limitation dynamics in north-east Greenland streams. Polar Research 37: 1–13.

Ensign, S. H. & M. W. Doyle, 2006. Nutrient spiraling in streams and river networks. Journal of Geophysical Research: Biogeosciences 1: 13.

Fisher, S. G., L. J. Gray, N. B. Grimm & D. E. Busch, 1982. Temporal succession in a desert stream ecosystem following flash flooding. Ecological Monographs 52: 93–110.

Fuller, M. R. & B. L. Peckarsky, 2011. Does the morphology of beaver ponds alter downstream ecosystems? Hydrobiologia 668: 35–48.

Gerull, L., A. Frossard, M. O. Gessner & M. Mutz, 2012. Effects of shallow and deep sediment disturbance on whole-stream metabolism in experimental sand-bed flumes. Hydrobiologia 683: 297–310.

Grimm, N. B., 1987. Nitrogen dynamics during succession in a desert stream. Ecology 68: 1157–1170.

Gu, L. Y. & K. H. Wyatt, 2016. Light availability regulates the response of algae and heterotrophic bacteria to elevated nutrient levels and warming in a northern boreal peatland. Freshwater Biology 61: 1442–1453.

Hall Jr., R. O. & J. L. Tank, 2003. Ecosystem metabolism controls nitrogen uptake in streams in Grand Teton National Park, Wyoming. Limnology and Oceanography 48: 1120–1128.

Hall Jr., R. O., M. A. Baker, C. D. Arp & B. J. Koch, 2009a. Hydrologic control of nitrogen removal, storage, and export in a mountain stream. Limnology and Oceanography 54: 2128–2142.

Hall Jr., R. O., J. L. Tank, D. J. Sobota, P. J. Mulholland, J. M. O'Brien, W. K. Dodds, J. R. Webster, H. M. Valett, G. C. Poole & B. J. Peterson, 2009b. Nitrate removal in stream ecosystems measured by 15 N addition experiments: total uptake. Limnology and Oceanography 54: 653–665.

Hanafi, S., M. R. Grace & B. T. Hart, 2006. Can Nutrient Spiralling be Used to Detect Seasonal Nutrient Uptake in a Forested Stream? Water, Air, & Soil Pollution: Focus 6: 403–411. https://doi.org/10.1007/s11267-006-9054-1.

Hanrahan, B. R., J. L. Tank, A. F. Aubeneau & D. Bolster, 2018. Substrate-specific biofilms control nutrient uptake in experimental streams. Freshwater Science 37: 456–471.

Harvey, J., J. Gomez-Velez, N. Schmadel, D. Scott, E. Boyer, R. Alexander, K. Eng, H. Golden, A. Kettner & C. Konrad, 2019. How hydrologic connectivity regulates water quality in river corridors. Journal of the American Water Resources Association 55: 369–381.

Holmes, R. M., A. Aminot, R. Kérouel, B. A. Hooker & B. J. Peterson, 1999. A simple and precise method for measuring ammonium in marine and freshwater ecosystems. Canadian Journal of Fisheries and Aquatic Sciences 56: 1801–1808.

Julian, J. P., M. W. Doyle & E. H. Stanley, 2008. Empirical modeling of light availability in rivers. Journal of Geophysical Research 113: 1–16.

Likens, G. E., F. H. Bormann, N. M. Johnson, D. W. Fisher & R. S. Pierce, 1970. Effects of forest cutting and herbicide treatment on nutrient budgets in the Hubbard Brook watershed-ecosystem. Ecological Monographs 40: 23–47.

Martí, E., N. B. Grimm & S. G. Fisher, 1997. Pre-and post-flood retention efficiency of nitrogen in a Sonoran Desert stream. Journal of the North American Benthological Society 16: 805–819.

Mueller Price, J., B. P. Bledsoe & D. W. Baker, 2015. Influences of sudden changes in discharge and physical stream characteristics on transient storage and nitrate uptake in an urban stream. Hydrological Processes 29: 1466–1479.

Mulholland, P. J., A. D. Steinman, A. V. Palumbo, D. L. DeAngelis & T. E. Flum, 1991. Influence of nutrients and grazing on the response of stream periphyton communities to a scour disturbance. Journal of the North American Benthological Society 10: 127–142.

Mulholland, P. J., A. D. Steinman, E. R. Marzolf, D. R. Hart & D. L. DeAngelis, 1994. Effect of periphyton biomass on hydraulic characteristics and nutrient cycling in streams. Oecologia 98: 40–47.

Mulholland, P. J., S. A. Thomas & H. M. Valett, 2006. Effects of light on NO3-uptake in small forested streams: diurnal and day-to-day variations. Journal of the North American Benthological Society 25: 583–595.

Mulholland, P. J., B. J. Roberts, W. R. Hill & J. G. Smith, 2009. Stream ecosystem responses to the 2007 spring freeze in the southeastern United States: unexpected effects of climate change. Global Change Biology 15: 1767–1776.

Murphy, J. & J. P. Riley, 1962. A modified single solution method for the determination of phosphate in natural waters. Analytica Chimica Acta 27: 31–36.

Ostrofsky, M. L. & F. H. Rigler, 1987. Chlorophyll–phosphorus relationships for subarctic lakes in western Canada. Canadian Journal of Fisheries and Aquatic Sciences 44: 775–781.

Passy, S. I. & C. A. Larson, 2011. Succession in stream biofilms is an environmentally driven gradient of stress tolerance. Microbial Ecology 62: 414–424.

Power, M. E., M. S. Parker & W. E. Dietrich, 2008. Seasonal reassembly of a river food web: floods, droughts, and impacts of fish. Ecological Monographs 78: 263–282.

Power, M. E., K. Bouma-Gregson, P. Higgins & S. M. Carlson, 2015. The Thirsty Eel: summer and Winter Flow Thresholds that Tilt the Eel River of Northwestern California from

Salmon-Supporting to Cyanobacterially Degraded States. Copeia 103: 200–211.
R Core Team. (2018). R: A language and environment for statistical computing. R Foundation for Statistical Computing, Vienna, Austria. https://www.Rproject.org/.
Reaman, M., 2017. Landslide Above Gothic Brings Brown Tint to the East River The Crested Butte News. Crested Butte News, Crested Butte.
Rosemond, A., 1993. Interactions among irradiance, nutrients, and herbivores constrain a stream algal community. Oecologia 94: 585–594.
Rueden, C. T., J. Schindelin, M. C. Hiner, B. E. DeZonia, A. E. Walter, E. T. Arena & K. W. Eliceiri, 2017. Image J2: ImageJ for the next generation of scientific image data. BMC Bioinformatics 18: 529–555.
Ryder, D. S., R. J. Watts, E. Nye & A. Burns, 2006. Can flow velocity regulate epixylic biofilm structure in a regulated floodplain river? Marine and Freshwater Research 57: 29–36.
Steiman, A., G. Lamberti & P. Leavitt, 2017. Biomass and pigments of benthic algae. In Hauer, F. R. & G. Lamberti (eds.), Methods in Stream Ecology, 3rd ed. Academic Press, Elsevier, London: 223–241.
Stewart, I. T., D. R. Cayan & M. D. Dettinger, 2005. Changes toward earlier streamflow timing across western North America. Journal of climate 18: 1136–1155.
Taylor, B. W., C. F. Keep, R. O. Hall Jr., B. J. Koch, L. M. Tronstad, A. S. Flecker & A. J. Ulseth, 2007. Improving the fluorometric ammonium method: matrix effects, background fluorescence, and standard additions. Journal of the North American Benthological Society 26: 167–177.
Triska, F. J., A. P. Jackman, J. H. Duff & R. J. Avanzino, 1994. Ammonium sorption to channel and riparian sediments: a transient storage pool for dissolved inorganic nitrogen. Biogeochemistry 26: 67–83.
Uehlinger, U. & M. W. Naegeli, 1998. Ecosystem metabolism, disturbance, and stability in a prealpine gravel bed river. Journal of the North American Benthological Society 17: 165–178.
Valett, H. M., C. L. Crenshaw & P. F. Wagner, 2002. Stream nutrient uptake, forest succession, and biogeochemical theory. Ecology 83: 2888–2901.
von Schiller, D., E. Martí, J. L. Riera, M. Ribot, A. Argerich, P. Fonollà & F. Sabater, 2008. Inter-annual, annual, and seasonal variation of P and N retention in a perennial and an intermittent stream. Ecosystems 11: 670–687.
Webster, J. R., P. J. Mulholland, J. L. Tank, H. M. Valett, W. K. Dodds, B. J. Peterson, W. B. Bowden, C. N. Dahm, S. Findlay & S. V. Gregory, 2003. Factors affecting ammonium uptake in streams – an inter-biome perspective. Freshwater Biology 48: 1329–1352.
Williams, M. W. & J. M. Melack, 1991. Solute chemistry of snowmelt and runoff in an alpine basin, Sierra Nevada. Water Resources Research 27: 1575–1588.
Williamson, T. J., W. F. Cross, J. P. Benstead, G. M. Gislason, J. M. Hood, A. D. Huryn, P. W. Johnson & J. R. Welter, 2016. Warming alters coupled carbon and nutrient cycles in experimental streams. Global Change Biology 22: 2152–2164.
Winnick, M. J., R. W. Carroll, K. H. Williams, R. M. Maxwell, W. Dong & K. Maher, 2017. Snowmelt controls on concentration-discharge relationships and the balance of oxidative and acid-base weathering fluxes in an alpine catchment, East River, Colorado. Water Resources Research 53: 2507–2523.
Yvon-Durocher, G., J. I. Jones, M. Trimmer, G. Woodward & J. M. Montoya, 2010. Warming alters the metabolic balance of ecosystems. Philsophical Transactions of the Royal Society B 365: 2117–2126.
Zhang, J. Z. & X. L. Huang, 2011. Effect of temperature and salinity on phosphate sorption on marine sediments. Environmental Science and Technology 45: 6831–6837.

Publisher's Note Springer Nature remains neutral with regard to jurisdictional claims in published maps and institutional affiliations.